ACS APPLIED MATERIALS & INTERFACES

Research Article

www.acsami.org

Silica–Titania Composite Aerogel Photocatalysts by Chemical Liquid Deposition of Titania onto Nanoporous Silica Scaffolds

Guoqing Zu,* Jun Shen,* Wenqin Wang, Liping Zou, Ya Lian, and Zhihua Zhang

Shanghai Key Laboratory of Special Artificial Microstructure Materials and Technology, Pohl Institute of Solid State Physics, Tongji University, Shanghai 200092, P. R. China

Supporting Information

ABSTRACT: Silica–titania composite aerogels were synthesized by chemical liquid deposition of titania onto nanoporous silica scaffolds. This novel deposition process was based on chemisorption of partially hydrolyzed titanium alkoxides from solution onto silica nanoparticle surfaces and subsequent hydrolysis and condensation to afford titania nanoparticles on the silica surface. The titania is homogeneously distributed in the silica–titania composite aerogels, and the titania content can be effectively controlled by regulating the deposition cycles. The resultant composite aerogel with 15 deposition cycles possessed a high specific surface area (SSA) of 425 m^2/g, a small particle size of 5–14 nm, and a large pore volume and pore size of 2.41 cm^3/g and 18.1 nm, respectively, after heat treatment at 600 °C and showed high photocatalytic activity in the photodegradation of methylene blue under UV-light irradiation. Its photocatalytic activity highly depends on the deposition cycles and heat treatment. The combination of small particle size, high SSA, and enhanced crystallinity after heat treatment at 600 °C contributes to the excellent photocatalytic property of the silica–titania composite aerogel. The higher SSAs compared to those of the reported titania aerogels (<200 m^2/g at 600 °C) at high temperatures combined with the simple method makes the silica–titania aerogels promising candidates as photocatalysts.

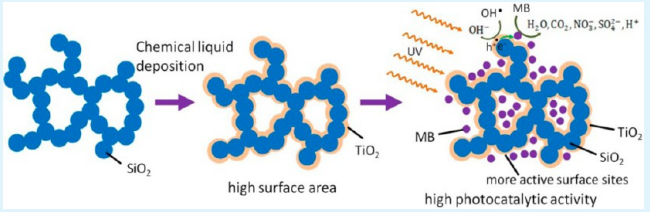

KEYWORDS: *silica–titania composite aerogel, sol–gel, chemical liquid deposition, photocatalyst, specific surface area*

1. INTRODUCTION

Titania nanomaterials are well-known for their excellent electrical, optical, and photocatalytic properties and have drawn great interest in a wide range of applications such as dye-sensitized solar cells,[1−3] water splitting,[4,5] high refractive optics,[6] oxide semiconductors,[7] oxygen sensors,[8] and photodegradation of organics.[9] One of the most attractive applications of titania materials is as photocatalysts for the removal of hazardous organic substances because of their strong oxidizing and reducing ability under UV-light irradiation.[10] There are mainly two factors affecting the photocatalytic activity of titania: specific surface area (SSA) and crystallinity. High SSA and crystallinity of anatase titania lead to a corresponding high photocatalytic activity. For this reason, many researchers have focused on nanoporous anatase titania to enhance the photocatalytic properties.[10−13]

As a kind of nanoporous material with high SSA, high porosity, and interconnective pores, titania aerogel becomes a promising candidate as a photocatalyst.[14,15] The optical and photocatalytic properties of titania itself combined with its small particle size and high SSA make titania aerogel an effective, environmentally friendly photocatalyst for the removal of nonbiodegradable pollutants normally present in air and wastewater via photocatalysis.

Titania aerogels are usually prepared by a sol–gel method and subsequent supercritical fluid drying without collapsing the networks. Although the as-prepared titania aerogel posseesses high SSAs up to 600–1000 m^2/g,[14,16] it shows poor crystallinity, which lowers its photocatalytic activity. While the crystallinity is enhanced by heat treatment at high temperatures, sintering occurs and its SSAs decrease drastically upon heat treatment. After heat treatment at 600 and 800 °C, the SSAs of pure titania aerogel are decreased to only 100–180 and 5–65 m^2/g, respectively.[16,17] It is believed that the heat resistance and SSAs at high temperatures can be enhanced by adding additives such as silica, alumina, or zirconia.[17−20] Many titania-based composite aerogels such as titania–silica, titania–alumina, and titania–zirconia aerogels are prepared by different methods.[17−22] Most of these composite methods are performed by the cogelation reaction of different precursors. Enhancement of the SSA is limited via this method. The SSA of titania–silica composite aerogel is decreased to ∼200 m^2/g after heat treatment at 800 °C.[17] The SSA of titania–alumina composite aerogel decreases to 84 m^2/g after heat treatment at 600 °C.[20] After the addition of zirconia via the cogelation method, the SSA increases to only 95 m^2/g at 800 °C.[21]

Composite aerogels can also be prepared by a deposition or modification method. Inorganic hollow nanotube aerogels have been prepared by atomic layer deposition onto native nanocellulose templates.[23] Atomic layer deposition or chemical

Received: December 18, 2014
Accepted: February 9, 2015
Published: February 9, 2015

DOI: 10.1021/am5089132
ACS Appl. Mater. Interfaces 2015, 7, 5400−5409

vapor deposition on pristine aerogels can afford robust composite aerogels.[24,25] Another method, namely, chemical liquid deposition method, is more convenient compared to the above two deposition methods owing to the lower temperature conditions. This method is widely used in the synthesis of nanostructured composite materials.[26−29] Malvadkar et al. have reported the chemical liquid deposition of titania onto nanostructured poly(*p*-xylylene) thin films and $MnCO_3$ microspheres with $(HN_4)_2TiF_6$ as the precursor.[28,29] The hydroxyl group on the nanoparticle surface of the silica wet gel makes it possible to be modified by chemical liquid deposition of organic precursors with hydroxyl groups, alkoxy groups, isocyanate, etc.[30−36] Many silica-based composite aerogels have been prepared via this deposition method. In this paper, silica−titania composite aerogels were synthesized for the first time by chemical liquid deposition of titania onto nanoporous silica scaffolds. The deposition process was based on chemisorption of partially hydrolyzed titanium alkoxides from solution onto nanoparticle surfaces of silica wet gels and subsequent hydrolysis and condensation to afford titania nanocoatings. It involves the following three steps. First, a silica wet gel monolith is immersed in a mixture of partially hydrolyzed titanium alkoxide and ethanol (EtOH). Second, it is immersed in a mixture of EtOH and a small amount of water. Third, it is washed with EtOH. These three steps are repeated 5−15 times. The optimized silica−titania composite aerogel possesses a high SSA of 425 m^2/g and a large pore volume and pore size of 2.41 cm^3/g and 18.1 nm, respectively, after heat treatment at 600 °C and shows high photocatalytic activity in the photodegradation of methylene blue under UV-light irradiation.

2. MATERIALS AND METHODS

Materials. Ethanol (EtOH), distilled water (H_2O), tetraethoxysilane (TEOS), titanium(IV) *n*-butoxide (TBO), HNO_3 (68%), HF (40%), and methylene blue (MB) were purchased from Sinopharm Chemical Reagent Corp. (China). All of the chemical reagents were used as received.

Preparation of Silica Wet Gels as Nanoporous Silica Scaffolds. The silica wet gel was prepared via a one-step sol−gel method with TEOS and HF as the precursor and catalyst, respectively. Appropriate amounts of TEOS, EtOH, and H_2O were mixed and stirred for 5 min, followed by the addition of HF to accelerate the hydrolysis and condensation reactions. The molar ratios of TEOS/EtOH/H_2O/HF used in the synthesis were 1:7.6:4:0.2. After stirring for 5 min, the mixture was poured into a glass beaker, where the gel typically formed within 1 h. The wet gel was then covered with a small amount of EtOH and aged for 2 days to strengthen the skeletal structure. Before chemical liquid deposition, solvent exchange with pure EtOH was performed in order to replace the pore solvent.

Chemical Liquid Deposition of Titania onto Nanoporous Silica Scaffolds. After solvent exchange for 2 days, the wet gel was coated with titania by immersion in a mixture of partially hydrolyzed titanium alkoxide and EtOH, a mixture of EtOH and H_2O, and EtOH in sequence, and the process was repeated for certain times. The deposition process involved the following three basic steps. First, a silica wet gel monolith was immersed in a mixture of partially hydrolyzed titanium alkoxide and EtOH for 2 h. Second, it was immersed in a mixture of EtOH and a small amount of H_2O for 2 h. Third, it was washed with pure EtOH for 1 h. These three steps were performed at 50 °C and repeated 5−15 times. The mixture of partially hydrolyzed titanium alkoxide and EtOH was prepared by mixing TBO, EtOH, H_2O, and HNO_3 in a molar ratio of TBO/EtOH/H_2O/HNO_3 = 1:120:1:0.053 and stirring for 10 min. The molar ratio of EtOH to H_2O in a mixture of EtOH and H_2O was kept at 60:1.

Supercritical Fluid Drying. The silica−titania composite wet gel was dried under supercritical conditions using EtOH as the drying agent. To meet the required conditions, the wet gel was placed in an autoclave partially filled with EtOH and sealed. Ultrapure dry nitrogen gas was flushed into the autoclave to reach an oxygen-free atmosphere and keep the initial pressure at 2 MPa. The autoclave temperature was then raised to 255 °C at a rate of 2 °C/min, while the pressure was controlled at ∼8 MPa. It was maintained at this temperature and pressure for 1 h, and the autoclave was then decompressed slowly at a rate of 30 kPa/min. Finally, the system was cooled to room temperature naturally, and the silica−titania composite aerogel was removed. The obtained silica−titania composite aerogels with deposition cycles of 5, 10, and 15 were denoted as SiO_2−TiO_2-5, SiO_2−TiO_2-10, and SiO_2−TiO_2-15, respectively.

These aerogels were heat-treated respectively at 400, 600, and 800 °C for 2 h in an air atmosphere in order to study the microstructure and photocatalytic properties at higher temperatures.

Characterization. The morphology of the sample was characterized by transmission electron microscopy (TEM; JEOL-1230) and scanning electron microscopy (SEM; XL30FEG, The Netherlands). TEM analysis was carried out at an acceleration voltage of 120 V. Energy-dispersive X-ray (EDX) elemental analysis was performed on the above scanning electron microscope. The surface functional groups of aerogels were investigated by Fourier transform infrared spectroscopy (FTIR; TENSOR27, Germany). The nature of the phases in the aerogels was analyzed by powder X-ray diffraction (XRD) in a Rigaku max-C diffractometer using Cu Kα radiation (DX-2700, China). The pore-size distribution, pore volume, and SSA were measured by a N_2 adsorption analyzer (TriStar 3000, USA) using the Brunauer−Emmett−Teller (BET) N_2 adsorption/desorption technique. The total pore volume was determined at P/P_0 = 0.98. The absorption spectra of a MB solution after UV-light irradiation (the output power was 250 W) in the presence of aerogels was measured by a UV/vis/near-IR (NIR) spectrophotometer (V-570, Japan).

3. RESULTS AND DISCUSSION

3.1. Chemical Liquid Deposition Method. Chemical liquid deposition in our work was performed through the reaction of the surface hydroxyl groups of silica wet gels with partially hydrolyzed precursors, namely, titanium alkoxides in the presence of a small amount of H_2O in liquid phase. The partially hydrolyzed precursor TBO could be expressed as $Ti(OH)_x(OC_4H_9)_{4-x}$. Because the molar ratio of the added H_2O to TBO is kept at 1:1, the value of x is presumed to be approximately 1.0. In the case of precipitation of the highly reactive TBO during deposition, appropriate amounts of HNO_3 are introduced in the mixture to stabilize TBO.[17] When the silica wet gel is immersed in a mixture of partially hydrolyzed TBO and EtOH, the partially hydrolyzed TBO would be adsorbed on the surface of the nanoparticles of the silica wet gel and react with the surface hydroxyl groups:After the wet gel is

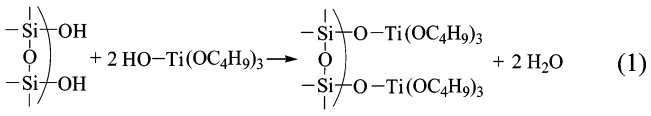

(1)

immersed in a mixture of EtOH and H_2O in the next step, hydrolysis and condensation of the adsorbed partially hydrolyzed TBO on the silica surface would take place:It should be

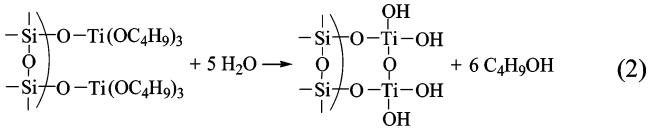

(2)

noted that only a small amount of H_2O is needed in the mixture of EtOH and H_2O. This is because the nanonetwork of

DOI: 10.1021/am5089132
ACS Appl. Mater. Interfaces 2015, 7, 5400−5409

silica wet gels would suffer cracking and the solvent exchange time would be prolonged in the presence of too much H_2O. The solvent exchange time is within 1 h, and there is no crack with 15 deposition cycles when the molar ratio of EtOH to H_2O is 60:1, whereas the solvent exchange needs more than 2 h and a few cracks appear in the wet gel with the same deposition cycles when the molar ratio decreases to 12:1. Repeating the deposition process would lead to the growth of titania nanoparticles and formation of titania nanocoatings on the silica surface and afford the silica–titania composite aerogel. The chemical liquid deposition process is schematically represented in Scheme 1.

Scheme 1. Schematic Representation of the Preparation of Silica–Titania Composite Aerogels via a Chemical Liquid Deposition Method

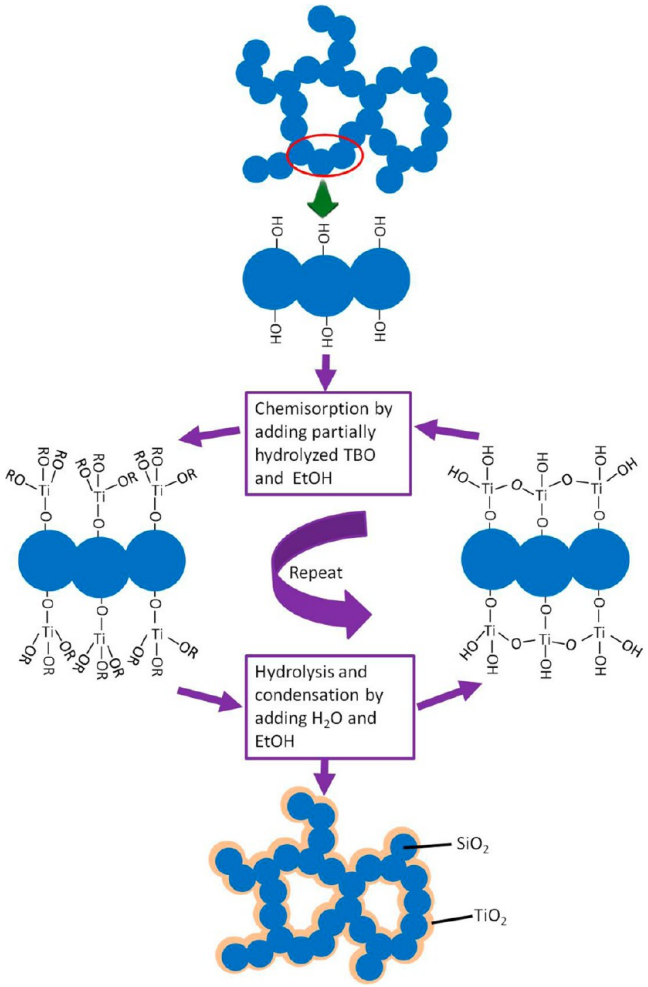

The deposited titania in the composite aerogels was confirmed by EDX elemental analysis (see Figure S1 in the Supporting Information, SI). The molar ratios of silica–titania in obtained composite aerogels were 9.2:1, 6.5:1, and 4.0:1 when the deposition cycles were 5, 10, and 15, respectively. This method can also be applied to the preparation of other porous silica–titania composites with higher loading amounts of TiO_2, which will be discussed in the future work. The composition of the silica–titania composite aerogels was further investigated, as can be seen from the FTIR spectra shown in Figure 1a. The peaks at 2965, 2926, 2858, and 1400 cm^{-1} for the as-prepared silica and silica–titania aerogels are attributed to the C–H bond,[37,38] which indicates that there are some residual carbonaceous organic groups in the aerogels after supercritical fluid drying. After heat treatment at 600 °C, these four peaks of the silica–titania composite aerogels vanish, which confirms that the organic groups linked to the network skeleton of the aerogels are eliminated by heat treatment at this temperature. For all of the samples, the intense band near 1100 cm^{-1} is assigned to three-dimensional Si–O–Si work asymmetric stretching vibrations.[39] The broad peak at around 1640 cm^{-1} is assigned to H–O–H bending vibrations of weakly bound H_2O adsorbed on the nanoparticle surface of aerogels.[40] According to the report, the band corresponding to Ti–O–Si vibrations is usually observed in the 950–960 cm^{-1} zone.[41] However, this band does not appear in the FTIR spectra, which is probably because it is covered by the band at 968 cm^{-1}, which corresponds to the Si–OH stretching vibration. It should be noted that a wide band between 750 and 500 cm^{-1} occurs after chemical liquid deposition and becomes more intense with more deposition cycles. The band at 750–500 cm^{-1} is attributed to the presence of titania and vibrations of Ti–O–Ti bonds.[18] This confirms that the content of titania in the composite aerogels becomes higher with an increase of the deposition cycles. Both the EDX elemental analysis and FTIR spectra confirm that the proportion of titania of the silica–titania composite aerogels can be effectively controlled by chemical liquid deposition.

In order to confirm whether titania is homogeneously distributed throughout the entire volume of the monolithic composite aerogels, the portions taken from the center and surface of the monolithic sample SiO_2–TiO_2-15 were analyzed by FTIR, as shown in Figure 1b. It can be seen that the spectra of the samples from the center and surface are overlapped, indicating that the concentrations of titania at the center and at the surface of the monolithic samples are similar. The composition is further confirmed by EDX analysis of sample SiO_2–TiO_2-15 from the center and surface of the monoliths (see Table S1 in the SI). The molar ratio of silica–titania in the center of the sample is 4.0:1, which is similar to that (3.9:1) in the surface. This confirms that titania is homogeneously distributed in the silica–titania composite aerogels.

3.2. Appearance and Morphology of Silica–Titania Composite Aerogels. The appearances of the silica–titania composite aerogels before and after heat treatment at different temperatures are shown in Figure 2. The as-prepared silica–titania composite aerogels after 15 deposition cycles (SiO_2–TiO_2-15) are opaque and light brown. The reason for the brown coloration is that there are residual carbonaceous organic groups in the composite aerogels after supercritical fluid drying, which is confirmed in the above analysis of FTIR. After heat treatment at 600 °C, the residual organic groups are eliminated, and the color of the composite aerogel then changes from brown to white, which is shown in Figure 2b. The reason for the silica–titania composite aerogel with 15 deposition cycles being opaque rather than transparent like silica aerogel is that more secondary particles will cluster together, forming larger domains (see Figure S2 in the SI) that promote light scattering and haziness. From Figure 2, we can also see shrinkage of the aerogels after heat treatment. Compared to the silica aerogel (~41%), the silica–titania composite aerogel (SiO_2–TiO_2-15) shows smaller volume shrinkage (~27%) after heat treatment at 800 °C. This indicates that the heat resistance

DOI: 10.1021/am5089132
ACS Appl. Mater. Interfaces 2015, 7, 5400–5409

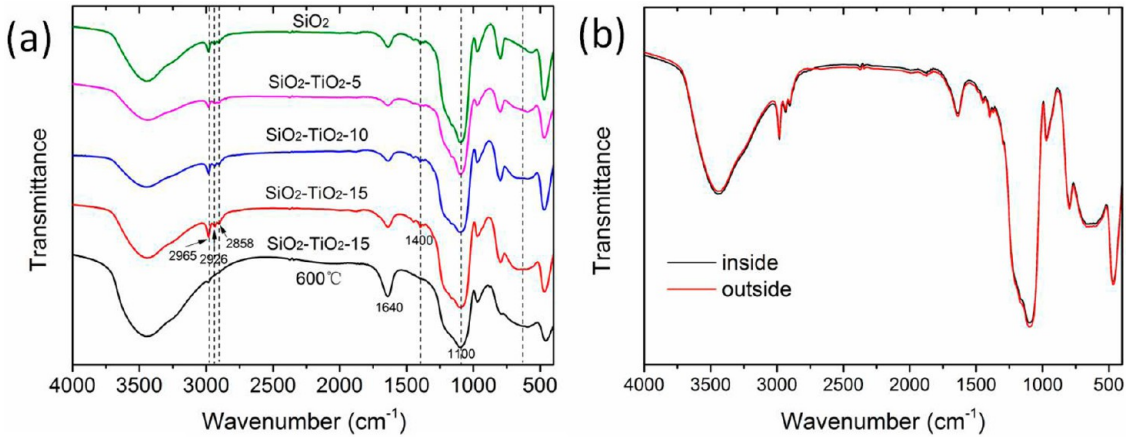

Figure 1. (a) FTIR spectra of silica and silica−titania composite aerogels. (b) FTIR spectra of the sample SiO_2−TiO_2-15 from the center and surface of the monoliths.

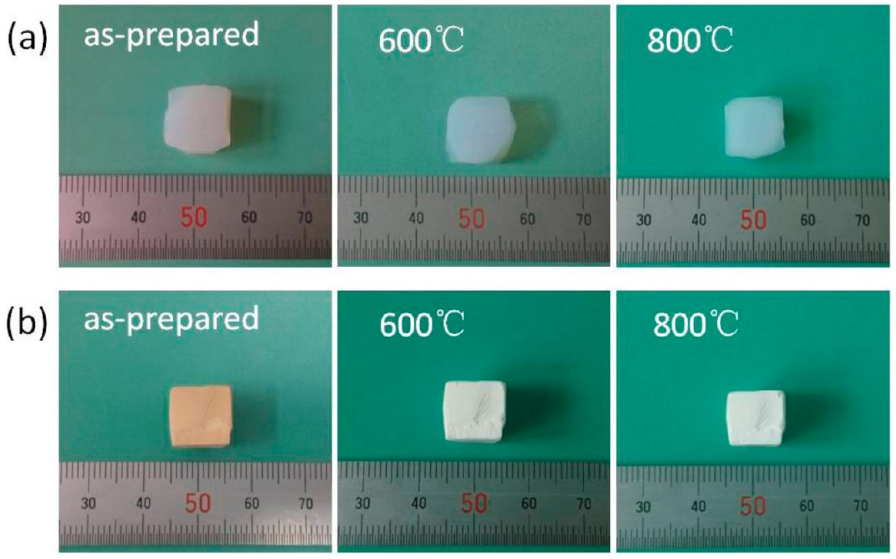

Figure 2. Photograph of typical aerogels before and after heat treatment at different temperatures: (a) SiO_2 aerogel; (b) SiO_2−TiO_2-15.

of the silica−titania composite aerogel is better than that of the silica aerogel.

The morphology of typical aerogels after heat treatment at 600 °C is shown in the TEM images (Figure 3). From the TEM images, we can see that both the silica and silica−titania composite aerogels exhibit interconnected networks made up of irregular sphere nanoparticles. It should be noted that the silica−titania composite aerogel shows larger and even clustered particles compared to that of the silica aerogel. The particle size of the silica aerogel is in range of 3.0−7.0 nm, whereas the particle size of the sample SiO_2−TiO_2-15 is in the range of 5.0−14.0 nm. The larger nanoparticles indicate that titania is deposited onto the surface of the silica scaffold after chemical liquid deposition. The observed particle growth is consistent with the reaction and cross-linking of TBO to the surface of silica. However, it should be noted that the particle size of the sample SiO_2−TiO_2-15 is much smaller than that of the nanoporous titania after heat treatment at 600 °C. It is reported that the mean crystal size of the nanoporous titania is increased up to 15 and ∼20 nm after heat treatment at 500 and 600 °C, respectively.[42,43] From Figure 3b−d, we can also see that, in spite of the growth of the nanoparticles, the silica−titania composite aerogels retain the nanoporous network structure. However, the TEM images of the silica−titania composite aerogels show some individual TiO_2 nanoparticles (which appear as dark spots) on the surface of the silica particles (which appear as white-gray areas), especially in the high TiO_2-loaded samples (SiO_2−TiO_2-10 and SiO_2−TiO_2-15). This is probably due to the following two reasons. First, the partially hydrolyzed TBO not only reacts with the hydroxyl groups on the silica surface but also condenses with other surrounding partially hydrolyzed TBO, which results in the growth of TiO_2 nanoparticles on the surface of silica particles. Second, H_2O may not be completely washed after washing with pure EtOH for 1 h, resulting in hydrolysis and condensation of the partially hydrolyzed TBO during deposition. In addition, the electron diffraction patterns in Figure 3 show that the silica−titania composite aerogels have several distinct reflections that are not observed in silica aerogel and the electron diffraction spot becomes stronger with an increase of the deposition cycles. This confirms that, different from the silica aerogel with an amorphous structure, the silica−titania composite aerogels exhibit polycrystalline structures and the crystallinity increases with an increase of the deposition cycles during chemical liquid deposition.

DOI: 10.1021/am5089132
ACS Appl. Mater. Interfaces 2015, 7, 5400−5409

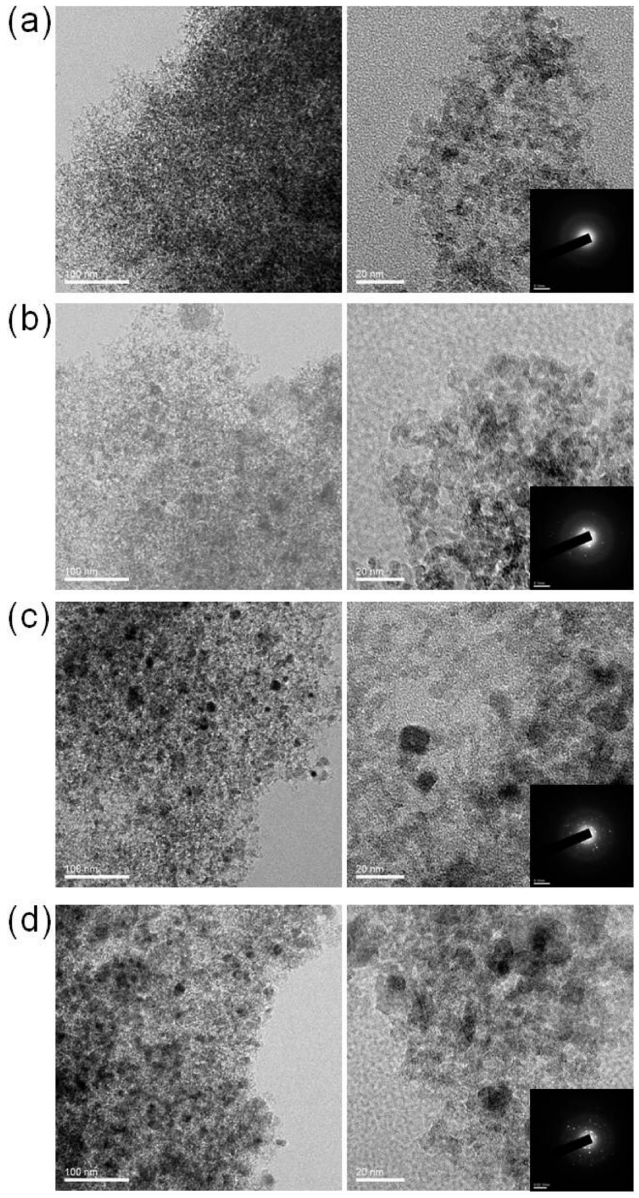

Figure 3. TEM images of the silica and silica–titania composite aerogels after heat treatment at 600 °C: (a) SiO_2 aerogel; (b) SiO_2–TiO_2-5; (c) SiO_2–TiO_2-10; (d) SiO_2–TiO_2-15. The insets are the corresponding electron diffraction patterns.

The hydrophobicity of the silica–titania composite aerogels is also different from that of the silica aerogel, which is shown in Figure 4. The as-prepared silica aerogel absorbs the drop of H_2O, and the structure in contact with H_2O is collapsed because of the capillary stress. However, the as-prepared SiO_2–TiO_2-15 does not collapse and allows the H_2O droplet to sit on the surface. When placed in H_2O, the as-prepared SiO_2–TiO_2-15 floats on top of H_2O, whereas the silica aerogel is fully immersed by H_2O and sinks to the bottom of the container. This indicates that, unlike the silica aerogel, which is hydrophilic, the as-prepared silica–titania composite aerogel is hydrophobic. The hydrophobicity is probably attributed to the hierarchical surface topography with combined microscale and nanoscale surface roughness by coating titania onto a nanoporous silica scaffold.[44] It should be noted that the silica–titania composite aerogel loses its hydrophobicity and becomes hydrophilic after heat treatment above 400 °C, which is

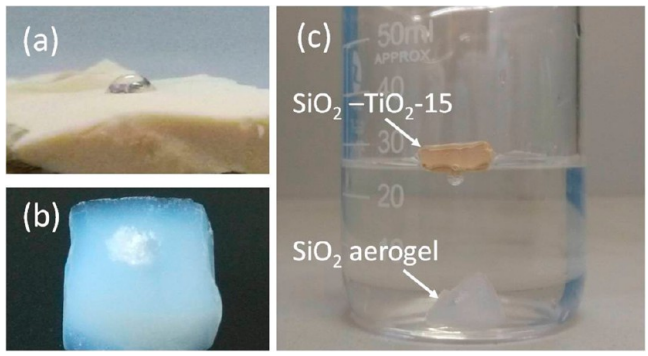

Figure 4. Images of the SiO_2 aerogel and SiO_2–TiO_2-15 when exposed to H_2O: (a) SiO_2–TiO_2-15 with the H_2O droplet on the surface; (b) SiO_2 aerogel with the adsorbed H_2O; (c) SiO_2 aerogel and SiO_2–TiO_2-15 that are placed in H_2O.

presumably because the rearrangement of the nanostructure at high temperatures changes the surface roughness of the nanoparticles.

3.3. Polycrystalline Structures. Figure 5a provides the XRD patterns for the silica aerogel and silica–titania composite aerogels with different deposition cycles after heat treatment at 600 °C. The silica aerogel is amorphous without any diffraction peaks, whereas the silica–titania composite aerogels exhibit broad diffraction peaks at 25°, 38°, 48°, 54°, 55°, 63°, 69°, 70°, and 75°, which correspond to (101), (004), (200), (105), (211), (204), (116), (220), and (215) reflection planes of anatase titania, respectively.[45] The broad peaks confirm the polycrystalline microstructure of the silica–titania composite aerogels. In addition, the deposition cycles of chemical liquid deposition effectively affect the polycrystalline structure of the resultant silica–titania composite aerogels. The peaks corresponding to the anatase phase become more intense with an increase of the deposition cycles, which indicates that more titania is deposited onto the silica surface with more deposition cycles during chemical liquid deposition. This result is consistent with the above TEM analysis. In addition, a high-resolution TEM image of sample SiO_2–TiO_2-15 after heat treatment at 600 °C is also provided, as shown in Figure 5b. The lattice fringes corresponding to the (101) reflection plane of anatase TiO_2 can be clearly observed, which confirms the incorporation of anatase TiO_2 in the composite aerogel.

The effect of heat treatment on the polycrystalline structure of the silica–titania aerogels is also investigated by XRD, which is shown in Figure 6. The as-prepared silica–titania composite aerogel SiO_2–TiO_2-15 gives very weak and broad peaks corresponding to the anatase phase. In contrast, the peaks are more intense and narrow after heat treatment at high temperatures ranging from 400 to 800 °C. This indicates that more anatase crystals are developed and the crystallinity of the silica–titania composite aerogels is effectively enhanced by heat treatment at high temperatures. In addition, no peaks of rutile occur for the silica–titania composite aerogel in the XRD patterns even after heat treatment at 800 °C.

3.4. SSA and Pore Structure. The SSA and pore structure are measured by a N_2 adsorption analyzer using the BET N_2 adsorption/desorption technique. The SSAs of typical aerogels are shown in Table 1. The SSA of the as-prepared aerogel decreases with an increase of the deposition cycles. The SSA is decreased from 613 m^2/g for the silica aerogel to 470 m^2/g for the sample SiO_2–TiO_2-15. The effect of heat treatment at high

DOI: 10.1021/am5089132
ACS Appl. Mater. Interfaces 2015, 7, 5400–5409

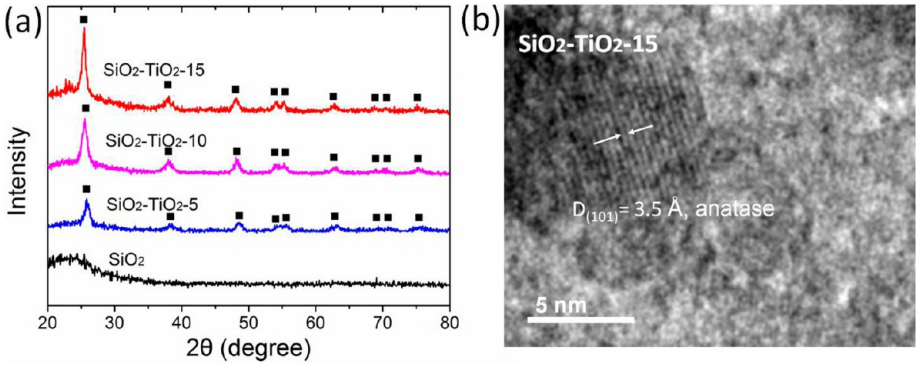

Figure 5. (a) XRD patterns for silica aerogel and silica−titania composite aerogels with different deposition cycles after heat treatment at 600 °C: (■) anatase TiO_2. (b) High-resolution TEM images of the sample SiO_2−TiO_2-15 after heat treatment at 600 °C.

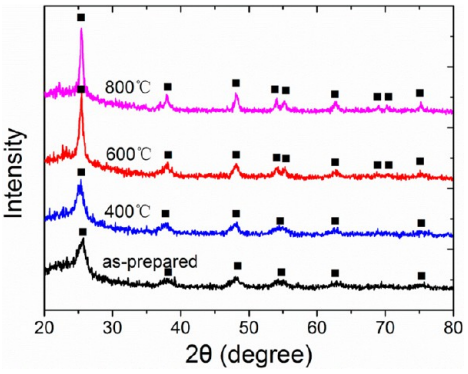

Figure 6. XRD patterns for the sample SiO_2−TiO_2-15 after heat treatment at different temperatures.

Table 1. Textural Properties of Typical Aerogels after Drying and after Heat Treatment at Different Temperatures

sample	temperature (°C)	S_{BET}[a] (m^2/g)	d[b] (nm)	V_p[c] (cm^3/g)
SiO_2	as-prepared	613	20.1	3.84
SiO_2−TiO_2-5	as-prepared	572	19.4	3.52
SiO_2−TiO_2-10	as-prepared	520	19.6	3.13
SiO_2−TiO_2-15	as-prepared	470	18.9	2.71
SiO_2−TiO_2-15	600	425	18.1	2.41
SiO_2−TiO_2-15	800	332	16.4	1.82

[a]BET SSA obtained from N_2 adsorption measurements. [b]Mean pore diameter obtained from the N_2 adsorption branch and Barrett−Joyner−Halenda. [c]Total pore volume.

temperatures on the SSA of the silica−titania composite aerogel is also investigated. The SSAs of the sample SiO_2−TiO_2-15 decrease to 425 and 332 m^2/g after heat treatment at 600 and 800 °C, respectively, for 2 h. The SSAs of the silica−titania composite aerogels are further compared to those of the reported titania and silica−titania aerogels. The SSAs of the pure titania aerogel are decreased to only 100−180 and 5−65 m^2/g after heat treatment at 600 and 800 °C, respectively.[16,17] The SSA of the titania−silica composite aerogel is decreased to ~200 m^2/g after heat treatment at 800 °C.[17] This indicates that, in spite of the decrease upon heat treatment, the SSAs of the silica−titania composite aerogels at 600−800 °C are much higher than those of the reported titania and silica−titania aerogels.

The pore size and pore volume of the silica−titania composite aerogels are also influenced by chemical liquid deposition and heat treatment. As is shown in Table 1 and Figure 7a, although the pore diameter does not exhibit significant changes, the total pore volume changes a lot with different deposition cycles. The mean pore diameter and total pore volume decrease from 20.1 nm and 3.84 cm^3/g for the silica aerogel to 18.9 nm and 2.71 cm^3/g, respectively, for the sample SiO_2−TiO_2-15. After heat treatment at 600 °C, the large mean pore diameter and total pore volume of 18.1 nm and 2.41 cm^3/g for the sample SiO_2−TiO_2-15 are retained, respectively. After heat treatment at 800 °C, the mean pore diameter and total pore volume further decrease to 16.4 nm and 1.82 cm^3/g, respectively. The N_2 adsorption/desorption isotherms of the silica aerogel and sample SiO_2−TiO_2-15 are additionally given in Figure 7b. It is clearly observed that both the silica aerogel and sample SiO_2−TiO_2-15 show type IV isotherms with distinct capillary condensation steps at a relative

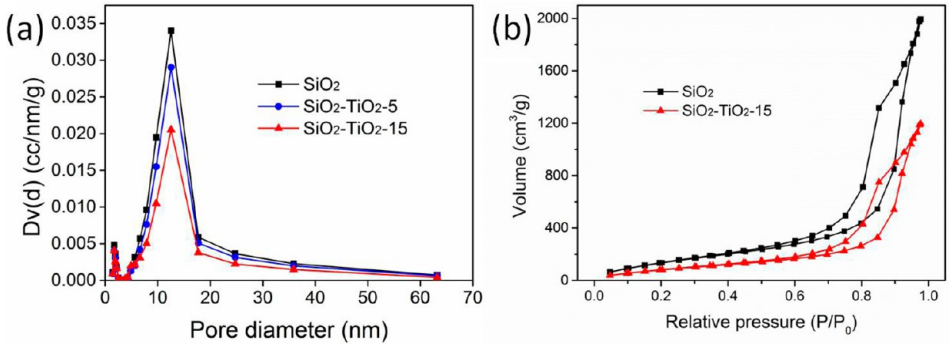

Figure 7. (a) Pore-size distributions and (b) N_2 adsorption/desorption isotherms for the silica aerogel and typical silica−titania composite aerogels.

DOI: 10.1021/am5089132
ACS Appl. Mater. Interfaces 2015, 7, 5400−5409

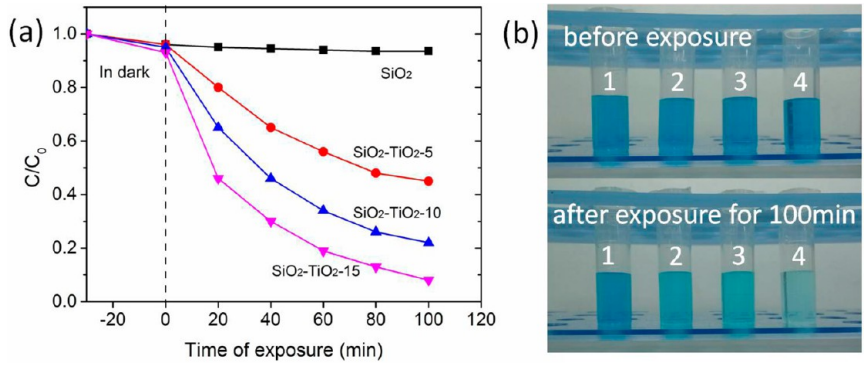

Figure 8. (a) Changes in the MB concentration percentage over the course of the photocatalytic degradation of MB in the presence of the different aerogels after heat treatment at 600 °C. The catalysis process was carried out under exposure to high-pressure fluorescent mercury lamp irradiation. (b) Photographs of the MB solution before and after exposure to irradiation for 100 min: (1) MB with silica aerogel; (2) MB with SiO_2−TiO_2-5; (3) MB with SiO_2−TiO_2-10; (4) MB with SiO_2−TiO_2-10. All of the aerogels were heat treated at 600 °C for 2 h and had equal weight.

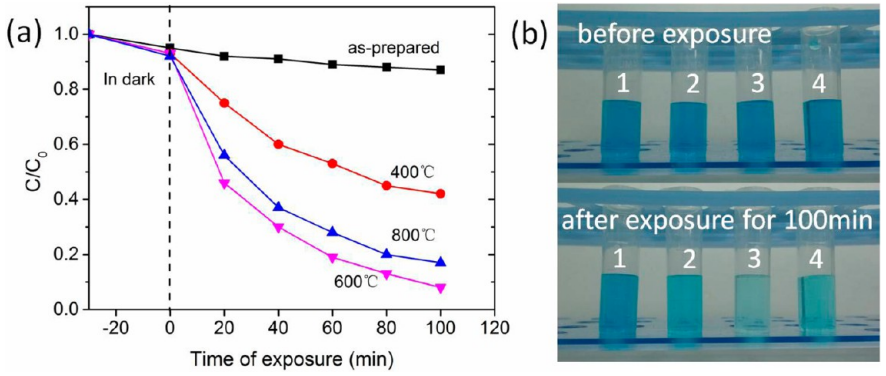

Figure 9. (a) Changes in the MB concentration percentage over the course of the photocatalytic degradation of MB in the presence of the sample SiO_2−TiO_2-15 before and after heat treatment at different temperatures. (b) Photographs of the MB solution before and after exposure to irradiation for 100 min in the presence of the sample SiO_2−TiO_2-15 (1) after drying and after heat treatment at (2) 400 °C, (3) 600 °C, and (4) 800 °C, respectively. All of the samples have equal weight.

pressure of 0.45−1.0, indicating that they are typical mesoporous materials with three-dimensional network structure.[46] To consider all of the pores in the mesoporous range, the isotherm should have a platform at high relative pressure. However, there is no obvious platform at high relative pressure in the isotherm, which would indicate that the pores are not completely filled and that the aerogels also have some larger pores except mesopores. Moreover, the nitrogen isotherms present a clear type H1 hysteresis loop, characterized by parallel and nearly vertical branches, which indicates that the composite aerogel consists of spherical particles.[47] The H1 hysteresis loops are also characteristic of materials with cylindrical pore geometry and a high degree of pore-size uniformity.[48,49] This confirms that the silica−titania composite aerogels own relatively high pore-size uniformity and facile pore connectivity.

The decrease of the SSA, pore diameter, and pore volume of the silica−titania composite aerogels compared to that of the silica aerogel is because nanoparticles grow larger and even cluster together after chemical liquid deposition (Figures 3 and S2 in the SI), which reduces mesopores as well as SSAs. The decrease of the SSA, pore diameter, and pore volume after heat treatment at 600 °C is mainly because the titania nanoparticles start to sinter at this temperature. The further decrease of the SSAs at 800 °C is due to the sintering of both silica and titania nanoparticles, which is confirmed by shrinkage of the composite aerogels shown in Figure 2.

3.5. Photocatalytic Properties. Owing to their high thermal stability, high SSA, small particle size, and large pore volume at high temperatures, the silica−titania composite aerogels are presumed to exhibit excellent photocatalytic properties. The photocatalytic properties of typical aerogels after heat treatment at 600 °C for degradation of MB are tested, as shown in Figure 8. The silica aerogel and silica−titania composite aerogel powders with equal weight (10 mg) were dispersed in several MB solutions with the same concentration (40 mL, 20 mg/L). The MB solutions with aerogels were stirred in the dark for adsorption for 30 min before UV-light irradiation. Photocatalytic degradation was then carried out by stirring the MB solutions with aerogels under a high-pressure mercury lamp. The absorption spectra of the MB solution in the presence of different aerogels for different exposure times were measured by a UV/vis/NIR spectrophotometer. After exposure for 100 min, the concentration percentage of MB with the silica aerogel remains 93%. Because the silica aerogel has no photocatalytic property, the small decrease of the concentration of MB is presumed to be attributed to the adsorption of the silica aerogel for MB. In contrast, the silica−titania composite aerogels exhibit photocatalytic activity in the photodegradation of MB under UV-light irradiation. After exposure for 100 min, the concentration percentages of MB with the samples SiO_2−TiO_2-5, SiO_2−TiO_2-10, and SiO_2−TiO_2-15 are 45%, 22%, and 8% respectively. In spite of the decrease of the SSA, the photocatalytic activity increases with more deposition cycles.

DOI: 10.1021/am5089132
ACS Appl. Mater. Interfaces 2015, 7, 5400−5409

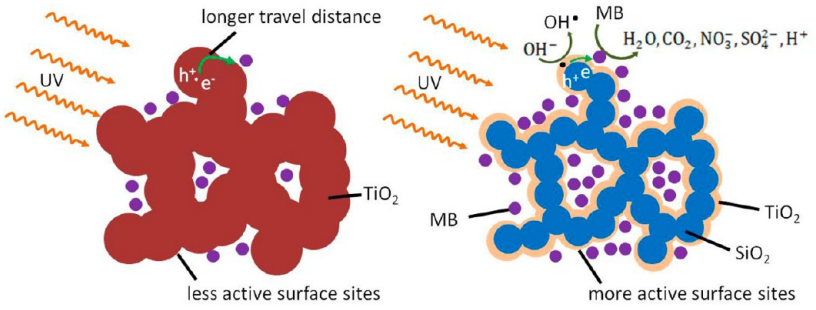

Figure 10. Schematic representation of the MB photocatalytic decomposition mechanism of the pure TiO_2 and silica–titania composite aerogels after heat treatment at 600 °C.

The enhanced photocatalytic property of the composite aerogels with more deposition cycles is attributed to the higher content of anatase titania in the composite aerogels with more deposition cycles, which is confirmed by the above EDX elemental analysis and FTIR.

The effect of heat treatment on the catalytic properties of the silica–titania composite aerogels is also studied by photocatalytic degradation of MB, which is shown in Figure 9. It can be seen that heat treatment significantly influences the photocatalytic activity. After exposure for 100 min, the concentration percentage of MB with the as-prepared sample SiO_2–TiO_2-15 remains 87%. By contrast, the concentration percentages of MB with the sample SiO_2–TiO_2-15 after heat treatment at 400 and 600 °C are much lower, namely, 42% and 8%, respectively. This could be explained as follows. More anatase crystals are developed and the crystallinity of the silica–titania composite aerogels is effectively enhanced by heat treatment at high temperatures, which is confirmed by XRD analysis. The enhanced crystallinity after heat treatment at 400 and 600 °C is probably responsible for the higher photocatalytic property of the silica–titania composite aerogels. However, after heat treatment at 800 °C for 2 h, the photocatalytic activity of sample SiO_2–TiO_2-15 declines. This is probably due to the sintering of the sample and the significant drop of the SSA (the SSA of the sample SiO_2–TiO_2-15 is decreased from 425 m^2/g at 600 °C to 332 m^2/g at 800 °C) at 800 °C. Among the samples in the test, the sample SiO_2–TiO_2-15 after heat treatment at 600 °C exhibits the best photocatalytic property for decomposition of MB.

The photocatalytic activity of the composite aerogel is compared to that of the commercial photocatalytic product Degussa P25. The photocatalytic test condition of Degussa P25 is the same as that of the composite aerogel. After exposure for 100 min, the concentration percentage of MB with Degussa P25 remains 37%, which is much higher than that with the sample SiO_2–TiO_2-15 after heat treatment at 600 °C (8%). This indicates that the sample SiO_2–TiO_2-15 after heat treatment at 600 °C shows much higher photocatalytic activity compared to that of Degussa P25. In addition, the photocatalytic efficiency of the optimized composite aerogel is better than that of the tubular structured hierarchical mesoporous titania material and similar to that of the titania–silica aerogel with titania as the dominant component prepared by a different method.[17,50] For the reported tubular titania material (5 mg), after being irradiated for 210 min, the MB (40 mL, 5 mg/L) remains 10%.[50] For the reported titania–silica aerogel (10 mg), after being irradiated for 80 min, the MB (40 mL, 20 mg/L) decreases to 6%.[17] The deposition process in our work is more simple, and a relatively lower titania content (10–20 wt %) is needed in the resultant materials, which makes this method more promising in the preparation of titania-based aerogel photocatalysts.

Furthermore, we theoretically discuss the mechanism of photocatalytic decomposition of MB using the silica–titania composite aerogels. When the MB solution with the composite aerogel is irradiated with UV light, the titania on the surface of the silica nanoparticles absorbs photons and generates electron–hole pairs because of ejection of an electron from the valence band into the conduction band, leaving behind a hole in the valence band:

$$TiO_2 + h\nu \rightarrow TiO_2 + e^- + h^+ \quad (3)$$

In contact with H_2O, the generated holes can react with H_2O and OH^- on the surface and form $OH^\bullet$ radicals:[13]

$$h^+ + H_2O \rightarrow H^+ + OH^\bullet \quad (4)$$

$$h^+ + OH^- \rightarrow OH^\bullet \quad (5)$$

The $OH^\bullet$ radicals can also be formed by the reaction of the generated electrons and protons with the dissolved oxygen. The radicals are able to oxidize MB to H_2O, carbon dioxide (CO_2), nitrate ions, sulfate ions, and protons:[43]

$$C_{16}H_{18}N_3S^+ + 102OH^\bullet \xrightarrow{UV,\ TiO_2} 57H_2O + 16CO_2 + 3NO_3^- + SO_4^{2-} + 6H^+ \quad (6)$$

In order to confirm the contribution of the hydroxyl radicals in the degradation reaction of MB, the sample SiO_2–TiO_2-15 is further tested by a similar photocatalytic experiment to verify hydroxyl radical production. The experimental conditions are the same except in the presence of tertiary butanol (*t*-BuOH; the volume ratio of *t*-BuOH to H_2O is 1:20) as a scavenger for hydroxyl radical species. After being irradiated for 100 min, MB remains 23%, which is higher than that without *t*-BuOH (8%). The photocatalytic activity shows an apparent decline after the introduction of a hydroxyl radical scavenger, confirming that hydroxyl radicals have a significant contribution in the degradation reaction of MB.

The mechanism of the photocatalytic decomposition of MB using the silica–titania composite aerogels is schematically represented in Figure 10. The efficiency of the decomposition of MB depends on the effectiveness of the photocatalytic process in transferring the e^-/h^+ pair from the particle volume to the particle surface and subsequently to the surface-adsorbed species. The e^-/h^+ pair may undergo volume and surface

DOI: 10.1021/am5089132
ACS Appl. Mater. Interfaces 2015, 7, 5400–5409

charge-carrier recombination and interfacial charge-transfer processes.[43] The small particle size (5.0−13.5 nm for SiO_2−TiO_2-15 after heat treatment at 600 °C) of the silica−titania composite aerogel results in a low volume charge-carrier recombination rate and a high interfacial charge-transfer rate, which guarantees the high photocatalytic activity. It should be noted that the titania particle size of the silica−titania composite aerogels increases and the photocatalytic activity is enhanced accordingly after heat treatment at 600 °C. This is consistent with the previous report that the photocatalytic activity of titania increases with larger particle size within a certain range (<15 nm for a reported porous nanocrystalline titania).[41,43] This is because relatively larger titania particles have greater effective surface area for greater photon absorption and electron−hole generation, leading to a better photocatalytic performance. On the other hand, the higher SSA (425 m^2/g for SiO_2−TiO_2-15 after heat treatment at 600 °C) of the composite aerogel compared to those of the reported titania and silica−titania aerogels increases the number of active surface sites and accelerates the diffusion of MB toward the reaction sites, which also enhances the interfacial charge-transfer rate. In addition, crystalline anatase particles are believed to be responsible for the production of reactive $OH^•$ radicals.[51] After heat treatment at high temperatures, the crystallinity of titania in the composite aerogel is enhanced and more anatase titania is produced, which leads to the enhanced productivity of $OH^•$ radicals. The combination of small particle size, high SSA, and enhanced crystallinity contributes to the excellent photocatalytic property of the sample SiO_2−TiO_2-15 after heat treatment at 600 °C.

4. CONCLUSIONS

In summary, we have demonstrated a novel method for the synthesis of silica−titania composite aerogels based on chemical liquid deposition on silica wet gels. The deposition in our work is performed through the reaction of the surface hydroxyl groups of silica wet gels with partially hydrolyzed titanium alkoxide precursors in the presence of a small amount of H_2O in liquid phase. The titania is homogeneously distributed in the silica−titania composite aerogels, and the titania content can be effectively controlled by regulating the deposition cycles. The optimized composite aerogel possessed a high SSA of 425 m^2/g and a large pore volume and pore size of 2.41 cm^3/g and 18.1 nm, respectively, after heat treatment at 600 °C. It also showed high photocatalytic activity in the photodegradation of MB under UV-light irradiation. The deposition cycles and heat treatment significantly affect its photocatalytic activity. Small particle size, high SSA, and enhanced crystallinity after heat treatment at 600 °C together contribute to the excellent photocatalytic property of the silica−titania composite aerogel. This chemical liquid deposition method could also be applied to prepare other composite aerogels such as silica−alumina, zirconia−titania, and silica−zirconia aerogels.

■ ASSOCIATED CONTENT

Supporting Information

EDX elemental analysis data, SEM images for typical aerogels, and element percentage of sample SiO_2-TiO_2-15. This material is available free of charge via the Internet at http://pubs.acs.org.

■ AUTHOR INFORMATION

Corresponding Authors

*E-mail: zuguoqing863@gmail.com.

*E-mail: shenjun67@tongji.edu.cn.

Notes

The authors declare no competing financial interest.

■ ACKNOWLEDGMENTS

We are thankful for financial support from the National Natural Science Foundation of China (Grants 51172163 and U1230113), National key Technology R&D Program of China (Grant 2013BAJ01B01), 863 Project of China, and Fundamental Research Funds for the Central Universities. We also are thankful for support from Bayer-Tongji Eco-Construction & Material Academy.

■ REFERENCES

(1) Mor, G. K.; Shankar, K.; Paulose, M.; Varghese, O. K.; Grimes, C. A. Use of Highly-Ordered TiO_2 Nanotube Arrays in Dye-Sensitized Solar Cells. *Nano Lett.* **2006**, *6*, 215−218.

(2) Kang, T. S.; Smith, A. P.; Taylor, B. E.; Durstock, M. F. Fabrication of Highly-Ordered TiO_2 Nanotube Arrays and Their Use in Dye-Sensitized Solar Cells. *Nano Lett.* **2009**, *9*, 601−606.

(3) Zhu, K.; Vinzant, T. B.; Neale, N. R.; Frank, A. J. Removing Structural Disorder from Oriented TiO_2 Nanotube Arrays: Reducing the Dimensionality of Transport and Recombination in Dye-Sensitized Solar Cells. *Nano Lett.* **2007**, *7*, 3739−3746.

(4) Osterloh, F. E. Inorganic Materials as Catalysts for Photochemical Splitting of Water. *Chem. Mater.* **2008**, *20*, 35−54.

(5) Mor, G. K.; Shankar, K.; Paulose, M.; Varghese, O. K.; Grimes, C. A. Enhanced Photocleavage of Water Using Titania Nanotube Arrays. *Nano Lett.* **2005**, *5*, 191−195.

(6) King, J. S.; Graugnard, E.; Summers, C. J. TiO_2 Inverse Opals Fabricated Using Low-Temperature Atomic Layer Deposition. *Adv. Mater.* **2005**, *17*, 1010−1013.

(7) Hoffmann, M. R.; Martin, S. T.; Choi, W.; Bahnemann, D. W. Environmental Applications of Semiconductor Photocatalysis. *Chem. Rev.* **1995**, *95*, 69−96.

(8) Morris, D.; Egdell, R. G. Application of V-Doped TiO_2 as a Sensor for Detection of SO_2. *J. Mater. Chem.* **2001**, *11*, 3207−3210.

(9) Chen, X. B.; Liu, L.; Yu, P. Y.; Mao, S. S. Increasing Solar Absorption for Photocatalysis with Black Hydrogenated Titanium Dioxide Nanocrystals. *Science* **2011**, *331*, 746−750.

(10) Shibata, H.; Ogura, T.; Mukai, T.; Ohkubo, T.; Sakai, H.; Abe, M. Direct Synthesis of Mesoporous Titania Particles Having a Crystalline Wall. *J. Am. Chem. Soc.* **2005**, *127*, 16396−16397.

(11) Liu, R.; Sen, A. Controlled Synthesis of Heterogeneous Metal−Titania Nanostructures and Their Applications. *J. Am. Chem. Soc.* **2012**, *134*, 17505−17512.

(12) Padmanabhan, S. C.; Pillai, S. C.; Colreavy, J.; Balakrishnan, S.; McCormack, D. E.; Perova, T. S.; Gunko, Y.; Hinder, S. J.; Kelly, J. M. A Simple Sol−Gel Processing for the Development of High-Temperature Stable Photoactive Anatase Titania. *Chem. Mater.* **2007**, *19*, 4474−4481.

(13) Pinho, L.; Mosquera, M. J. Titania−Silica Nanocomposite Photocatalysts with Application in Stone Self-Cleaning. *J. Phys. Chem. C* **2011**, *115*, 22851−22862.

(14) Stengl, V.; Bakardjieva, S.; Subrt, J.; Szatmary, L. Titania Aerogel Prepared by Low Temperature Supercritical Drying. *Microporous Mesoporous Mater.* **2006**, *91*, 1−6.

(15) Lin, C.-C.; Wei, T.-Y.; Lee, K.-T.; Lu, S.-Y. Titania and Pt/Titania Aerogels as Superior Mesoporous Structures for Photocatalytic Water Splitting. *J. Mater. Chem.* **2011**, *21*, 12668−12674.

(16) Campbell, L. K.; Na, B. K.; Ko, E. I. Synthesis and Characterization of Titania Aerogels. *Chem. Mater.* **1992**, *4*, 1329−1333.

(17) Zu, G.; Shen, J.; Wang, W.; Zou, L.; Lian, Y.; Zhang, Z.; Liu, B.; Zhang, F. Robust, Highly Thermally Stable, Core−Shell Nanostructured Metal Oxide Aerogels as High-Temperature Thermal

DOI: 10.1021/am5089132
ACS Appl. Mater. Interfaces 2015, 7, 5400−5409

Superinsulators, Adsorbents and Catalysts. *Chem. Mater.* **2014**, *26*, 5761−5772.
(18) Heiligtag, F. J.; Kranzlin, N.; Suess, M. J.; Niederberger, M. Anatase−Silica Composite Aerogels: a Nanoparticle-Based Approach. *J. Sol−Gel Sci. Technol.* **2014**, *70*, 300−306.
(19) Grunwaldt, J. D.; Beck, C.; Stark, W.; Hagen, A.; Baiker, A. In Situ XANES Study on TiO_2−SiO_2 Aerogels and Flame Made Materials. *Phys. Chem. Chem. Phys.* **2002**, *4*, 3514−3521.
(20) Subramanian, V.; Ni, Z.; Seebauer, E. G.; Masel, R. I. Synthesis of High-Temperature Titania−Alumina Supports. *Ind. Eng. Chem. Res.* **2006**, *45*, 3815−3820.
(21) Wan, Y.; Ma, J.; Zhou, W.; Zhu, Y.; Song, X.; Li, H. Preparation of Titania−Zirconia Composite Aerogel Material by Sol−Gel Combined with Supercritical Fluid Drying. *Appl. Catal., A* **2004**, *277*, 55−59.
(22) Torma, V.; Peterlik, H.; Bauer, U.; Rupp, W.; Husing, N.; Bernstorff, S.; Steinhart, M.; Goerigk, G.; Schubert, U. Mixed Silica Titania Materials Prepared from a Single-Source Sol−Gel Precursor: A Time-Resolved SAXS Study of the Gelation, Aging, Supercritical Drying, and Calcination Processes. *Chem. Mater.* **2005**, *17*, 3146−3153.
(23) Korhonen, J. T.; Hiekkataipale, P.; Malm, J.; Karppinen, M.; Illala, O.; Ras, R. H. A. Inorganic Hollow Nanotube Aerogels by Atomic Layer Deposition onto Native Nanocellulose Templates. *ACS Nano* **2011**, *5*, 1967−1974.
(24) Shin, S. J.; Tran, I. C.; Willey, T. M.; Buuren, T.; Ilavsky, J.; Biener, M. M.; Worsley, M. A.; Hamza, A. V.; Kucheyev, S. O. Robust Nanoporous Alumina Monoliths by Atomic Layer Deposition on Low-Density Carbon-Nanotube Scaffolds. *Carbon* **2014**, *73*, 443−447.
(25) Boday, D. J.; DeFriend, K. A.; Wilson, K. V., Jr.; Coder, D.; Loy, D. A. Formation of Polycyanoacrylate−Silica Nanocomposites by Chemical Vapor Deposition of Cyanoacrylates on Aerogels. *Chem. Mater.* **2008**, *20*, 2845−2847.
(26) Higuchi, R.; Tanoue, R.; Enoki, N.; Miyasato, Y.; Sakaguchi, K.; Uemura, S.; Kimizuka, N.; Kunitake, M. Chemical Liquid Deposition of Aromatic Poly(azomethine)s by Spontaneous On-Site Polycondensation in Aqueous Solution. *Chem. Commun.* **2012**, *48*, 3103−3105.
(27) Barriere, C.; Alcaraz, G.; Margeat, O.; Fau, P.; Quoirin, J. B.; Anceau, C.; Chaudret, B. Copper Nanoparticles and Organometallic Chemical Liquid Deposition (OMCLD) for Substrate Metallization. *J. Mater. Chem.* **2008**, *18*, 3084−3086.
(28) Malvadkar, N.; Dressick, W. J.; Demirel, M. C. Liquid Phase Deposition of Titania onto Nanostructured Poly-*p*-xylylene Thin Films. *J. Mater. Chem.* **2009**, *19*, 4796−4804.
(29) Lee, H. K.; Sakemi, D.; Selyanchyn, R.; Lee, C. G.; Lee, S. W. Titania Nanocoating on $MnCO_3$ Microspheres via Liquid-Phase Deposition for Fabrication of Template-Assisted Core−Shell- and Hollow-Structured Composites. *ACS Appl. Mater. Interfaces* **2014**, *6*, 57−64.
(30) Leventis, N. Three-Dimensional Core-Shell Superstructures: Mechanically Strong Aerogels. *Acc. Chem. Res.* **2007**, *40*, 874−884.
(31) Mohite, D. P.; Larimore, Z. J.; Lu, H.; Mang, J. T.; Sotiriou-Leventis, C.; Leventis, N. Monolithic Hierarchical Fractal Assemblies of Silica Nanoparticles Cross-Linked with Polynorbornene via ROMP: A Structure−Property Correlation from Molecular to Bulk through Nano. *Chem. Mater.* **2012**, *24*, 3434−3448.
(32) Leventis, N.; Leventis, C. S.; Zhang, G.; Rawashdeh, A. M. M. Nanoengineering Strong Silica Aerogels. *Nano Lett.* **2002**, *2*, 957−960.
(33) Wang, Z.; Dai, Z.; Wu, J.; Zhao, N.; Xu, J. Vacuum-Dried Robust Bridged Silsesquioxane Aerogels. *Adv. Mater.* **2013**, *25*, 4494−4497.
(34) Randall, J. P.; Meador, M. A. B.; Jana, S. C. Tailoring Mechanical Properties of Aerogels for Aerospace Applications. *ACS Appl. Mater. Interfaces* **2011**, *3*, 613−626.
(35) Sanli, D.; Erkey, C. Monolithic Composites of Silica Aerogels by Reactive Supercritical Deposition of Hydroxy-Terminated Poly(Dimethylsiloxane). *ACS Appl. Mater. Interfaces* **2013**, *5*, 11708−11717.
(36) Franzel, L.; Wingfield, C.; Bertino, M. F.; Mahadik-Khanolkar, S.; Leventis, N. Regioselective Cross-Linking of Silica Aerogels with Magnesium Silicate Ceramics. *J. Mater. Chem. A* **2013**, *1*, 6021−6029.
(37) Zu, G.; Shen, J.; Wei, X.; Ni, X.; Zhang, Z.; Wang, J.; Liu, G. Preparation and Characterization of Monolithic Alumina Aerogels. *J. Non-Cryst. Solids* **2011**, *357*, 2903−2906.
(38) Zu, G.; Shen, J.; Zou, L.; Wang, W.; Lian, Y.; Zhang, Z.; Du, A. Nanoengineering Super Heat-Resistant, Strong Alumina Aerogels. *Chem. Mater.* **2013**, *25*, 4757−4764.
(39) Zelenak, V.; Hornebecq, V.; Mornet, S.; Schaf, O.; Llewellyn, P. Mesoporous Silica Modified with Titania: Structure and Thermal Stability. *Chem. Mater.* **2006**, *18*, 3184−3191.
(40) Li, G. S.; Li, L. P.; Boerio-Goates, J.; Woodfield, B. F. High Purity Anatase TiO_2 Nanocrystals: Near Room-Temperature Synthesis, Grain Growth Kinetics, and Surface Hydration Chemistry. *J. Am. Chem. Soc.* **2005**, *127*, 8659−8666.
(41) Pinho, L.; Mosquera, M. J. Photocatalytic Activity of TiO_2−SiO_2 Nanocomposites Applied to Buildings: Influence of Particle Size and Loading. *Appl. Catal., B* **2013**, *134*−*135*, 205−221.
(42) Wu, N. L.; Wang, S. Y.; Rusakova, I. A. Inhibition of Crystallite Growth in the Sol−Gel Synthesis of Nanocrystalline Metal Oxides. *Science* **1999**, *285*, 1375−1377.
(43) Baiju, K. V.; Shukla, S.; Sandhya, K. S.; James, J.; Warrier, K. G. K. Photocatalytic Activity of Sol−Gel-Derived Nanocrystalline Titania. *J. Phys. Chem. C* **2007**, *111*, 7612−7622.
(44) Kettunen, M.; Silvennoinen, R. J.; Houbenov, H.; Nykanen, A.; Ruokolainen, J.; Sainio, J.; Pore, V.; Kemell, M.; Ankerfors, M.; Lindstrom, T.; Ritala, M.; Ras, R. H. A.; Ikkala, O. Photoswitchable Superabsorbency Based on Nanocellulose Aerogels. *Adv. Funct. Mater.* **2011**, *21*, 510−517.
(45) Chou, T. P.; Zhang, Q.; Russo, B.; Fryxell, G. E.; Cao, G. Titania Particle Size Effect on the Overall Performance of Dye-Sensitized Solar Cells. *J. Phys. Chem. C* **2007**, *111*, 6296−6302.
(46) Kong, Y.; Jiang, G.; Fan, M.; Shen, X.; Cui, S.; Russell, A. G. A New Aerogel Based CO_2 Adsorbent Developed Using a Simple Sol−Gel Method along with Supercritical Drying. *Chem. Commun.* **2014**, *50*, 12158−12161.
(47) Kruk, M.; Jaroniec, M. Gas Adsorption Characterization of Ordered Organic−Inorganic Nanocomposite Materials. *Chem. Mater.* **2001**, *13*, 3169−3183.
(48) Huo, Q.; Margolese, D. I.; Stucky, G. D. Surfactant Control of Phases in the Synthesis of Mesoporous Silica-Based Materials. *Chem. Mater.* **1996**, *8*, 1147−1160.
(49) Kruk, M.; Jaroniec, M. Application of Large Pore MCM-41 Molecular Sieves to Improve Pore Size Analysis Using Nitrogen Adsorption Measurements. *Langmuir* **1997**, *13*, 6267−6273.
(50) Huang, H.; Liu, X.; Huang, J. Tubular Structured Hierarchical Mesoporous Titania Material Derived from Natural Cellulosic Substances and Application as Photocatalyst for Degradation of Methylene Blue. *Mater. Res. Bull.* **2011**, *46*, 1814−1818.
(51) Ismail, A. A.; Bahnemann, D. W.; Robben, L.; Yarovyi, V.; Wark, M. Palladium Doped Porous Titania Photocatalysts: Impact of Mesoporous Order and Crystallinity. *Chem. Mater.* **2010**, *22*, 108−116.

DOI: 10.1021/am5089132
ACS Appl. Mater. Interfaces 2015, 7, 5400−5409